

Chrono🕒: A Simple Blueprint for Representing Time in MLLMs

Boris Meinardus^{1,2} Hector Rodriguez Garcia² Anil Barta³ Anna Rohrbach² Marcus Rohrbach²

Abstract

The recent success of Large Language Models (LLMs) has prompted the extension to the multi-modal domain developing image-text Multimodal LLMs (MLLMs) and then video-text models. In this work, we investigate the challenge of contextual and temporal comprehension in video-language models by exploring the task of *temporal localization* in videos. To address this problem, prior works have developed complex task-specific architectures, novel modules to embed time into MLLMs, or leveraged additional input signals such as video transcripts to best encode contextual and temporal information. Interestingly, we find that most of these efforts are surpassed by a much simpler design. We introduce *Chrono*🕒, a universal sequence blueprint that can be applied to an image-text pretrained MLLM. Through extensive ablations across different MLLM architectures, finetuning and zero-shot settings, and different datasets, we achieve a new SOTA in moment retrieval on the most widely used benchmarks Charades-STA, QVHighlights, ActivityNet Captions, and grounded video question answering on NeXT-GQA.⁴

1. Introduction

The recent success of pretrained large language models (LLMs) (Brown et al., 2020; Zhang et al., 2022; Chung et al., 2022) has inspired the development of generative image-text pretrained multimodal large language models (MLLMs) (Alayrac et al., 2022; Li et al., 2023; Huang et al., 2024b) that can comprehend vision and language modalities jointly. However, due to higher computational and annotation costs, large-scale pretraining on video data is more challenging to scale. To circumvent the issue, recent studies

¹TU Berlin, Berlin, Germany ²TU Darmstadt & Hessian.ai, Darmstadt, Germany ³University of Edinburgh, UK. Correspondence to: Boris Meinardus <boris.meinardus00@gmail.com>.

⁴Our code is available under <https://github.com/sudo-Boris/mr-Blip>.

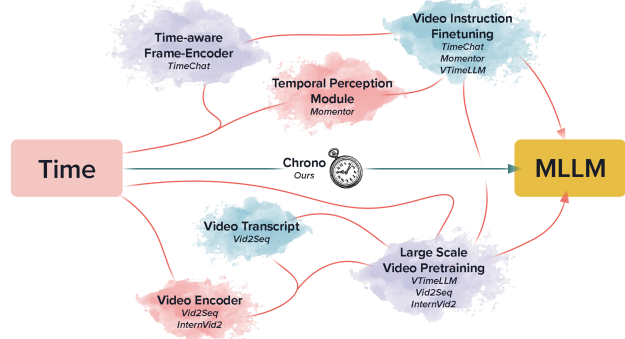


Figure 1. **How can we endow an MLLM with a sense of time?** In contrast to prior work, which leverages separate modules and diverse pretraining strategies, *Chrono*🕒 natively allows the MLLM to understand the language of time and associate it with the corresponding segments in a video.

leverage image-text pretrained models for image-to-video transfer learning (Yu et al., 2023; 2024; Lei et al., 2021b; Luo et al., 2022; Fang et al., 2021; Ju et al., 2022). Such models offer promising results in the direction of video-text retrieval (Luo et al., 2022), video captioning (Xu et al., 2023), or multiple choice video question answering (Yu et al., 2024). Yet, those tasks don’t require precise temporal understanding, whereas the task of *moment retrieval* (MR) requires the precise temporal localization of all moments associated with an open-ended natural-language query in an untrimmed video and has not been extensively explored.

This task has multiple potential valuable applications, such as video search or video indexing, but most importantly, it can be leveraged as a testing bed for a concrete temporal understanding of video-language models. More concretely, it requires understanding, discrimination, and temporal localization of multiple events in potentially minutes-long videos given an open-ended natural-language query. In the context of MLLMs, it is an open question of how to best model this task as a sequence-to-sequence prediction task, specifically, how to encode time best so the model can reason about it and predict start and end timestamps correctly.

Traditionally, prior works generally approach the challenge of moment retrieval by leveraging video features (Feichten-

hofer et al., 2019) or CLIP (Radford et al., 2021) to train a complex, task-specific feature fusion module, which ultimately predicts a fixed set of candidates. As shown in Figure 1, recent and concurrent approaches employ MLLMs for temporally grounded video-language tasks, one of the most relevant being moment retrieval. However, they often require large-scale instruction tuning datasets (Ren et al., 2023; Qian et al., 2024; Yang et al., 2023), complex multi-stage training (Huang et al., 2024a), specialized architectures (Qian et al., 2024; Ren et al., 2023), or further input signal, such as video transcripts (Yang et al., 2023).

In contrast, we develop *Chrono*[Ⓢ], a novel multi-modal input sequence blueprint that can enable image-text pretrained MLLMs to perform video moment retrieval. Interestingly, our thorough ablations demonstrate that our simple approach outperforms all prior methods, which add significantly more complexity, as shown in Figure 1. We show that this input design enables the best temporal grounding abilities both when finetuning image-text pretrained MLLMs or when using powerful MLLMs for zero-shot applications. Our approach achieves state-of-the-art (SOTA) results across the widely used benchmarks Charades-STA (Gao et al., 2017), QVHighlights (Lei et al., 2021a), and ActivityNet Captions (Krishna et al., 2017). We discuss the relevance of deliberate design choices by conducting extensive ablation studies on two MLLM backbones with different architectures, BLIP-2 (Li et al., 2023) and GPT-4o (OpenAI, 2024a). Besides the video moment retrieval datasets, we also consider NExT-GQA (Xiao et al., 2023), a dataset for grounded video QA (GVQA). The task there is to localize temporal segment(s) relevant to the question’s answer. Here, we assess *Chrono*’s ability to localize such video evidence without being trained for this task, as well as to generate an answer; again, we achieve SOTA results.

Our main contributions are as follows: (i) We leverage image-text pretrained MLLMs to approach moment retrieval by casting it as an open-ended sequence-to-sequence problem. (ii) To enhance the temporal understanding of events in input videos, we design a novel multimodal input sequence and introduce *Chrono*[Ⓢ], a simple and universal blueprint for representing time in MLLMs. (iii) *Chrono* models improve the state-of-the-art on the widely used moment retrieval benchmarks (Gao et al., 2017; Lei et al., 2021a; Krishna et al., 2017) and achieves a new SOTA on grounded VQA (Xiao et al., 2023). (iv) Extensive experiments and ablations demonstrate the effectiveness of *Chrono* and its design choices, highlighting that deliberate exploration of simple methods can outperform complex, potentially over-engineered methods. (v) We make our code and models publicly available.

2. Related Work

2.1. Moment Retrieval Models

Moment Retrieval analyzes an untrimmed video and aims to find the relevant clip for a given open-ended natural language query. Conventional approaches fall into either proposal-based or proposal-free methods. Proposal-based methods learn to identify moment candidates given predefined proposals, e.g., sliding windows (Anne Hendricks et al., 2017; Gao et al., 2017) and temporal anchors (Chen et al., 2018; Wang et al., 2020), in a first stage. In a second stage, these candidates are further refined to better match the text query. Regression-based methods (Lei et al., 2021a; Yan et al., 2023; Liu et al., 2022; Mun et al., 2020; Zeng et al., 2020) are common among proposal-free approaches. These directly predict the temporal boundaries of a relevant moment, without needing a first stage to generate initial proposals. Nevertheless, proposal-free methods still predict a fixed number of candidate windows alongside a confidence score, based on which the predictions are sorted. Using a fixed number of proposals has some downsides, like not generalizing to videos with a higher number of actions than the data used for tuning the number of proposals hyperparameter or wasted computation on duplicate proposals.

Recent works have explored various approaches to temporal modeling using multimodal LLMs. Ren et al. (2023) introduce time-sensitive frame embeddings by incorporating temporal information through Q-Former, into their model, TimeChat. Huang et al. (2024a) train VTimeLLM in a three-stage training setup, including extensive video-language pretraining. Momentor (Qian et al., 2024) proposes a dedicated Temporal Perception Module, and Lita (Huang et al., 2025) explores special temporal tokens. While these recent and in various cases concurrent approaches demonstrate the potential of MLLMs for temporal understanding, they often require large-scale instruction tuning datasets (TimeChat, Momentor), complex multi-stage training (VTimeLLM), or specialized architectures (Momentor). In contrast, our work shows that careful design choices in representing temporal information can enable moment retrieval without any prior training on the moment retrieval task. Furthermore, when combined with direct finetuning on downstream tasks, our *Chrono*[Ⓢ] blueprint can achieve superior performance without the need for expensive pretraining or architectural complexity. Through systematic ablations, we demonstrate that simple design choices - such as using absolute integer timestamps - can outperform more complex approaches that introduce special tokens or dedicated temporal modules.

2.2. Image-to-Video Transfer Learning

The limited public availability of high-quality large-scale video-language datasets, together with the immense compute requirements of training using videos, pose a signifi-

cant challenge for large-scale video-language pretraining. The idea of leveraging image-language pretrained models for image-to-video transfer learning by utilizing a limited number of video frames to enhance learning efficiency has proven effective as evidenced by many recent publications (Yu et al., 2023; 2024; Cao et al., 2022; Fang et al., 2021; 2022; Ju et al., 2022; Lei et al., 2021b; Luo et al., 2022; Ma et al., 2022; Lei et al., 2022; Xue et al., 2023; Wang et al., 2022). In particular, (Yu et al., 2024) makes use of the contextual understanding of MLLMs to perform video QA tasks. The authors train a BLIP-2 model to individually select 4 question-relevant frames and, using those, finetune another BLIP-2 to answer the question. We also leverage the pretrained BLIP-2 model and finetune it on the downstream task of moment retrieval, achieving big localization improvements over Yu et al. (2024). Furthermore, we show that strong image-text models like GPT-4o (OpenAI, 2024b), which cannot perform moment retrieval natively, achieve competitive results using our *Chrono* blueprint.

3. Chrono 🕒

To explore how to best represent time in an MLLM, we select the task of moment retrieval as a suitable test bed. The task is to temporally localize all relevant moments in an untrimmed video given an open-ended natural language query. Therefore, a key challenge is to effectively model the contextual and temporal relationship between the different events in the video, for example, as illustrated in Figure 2, a man is talking to the camera followed by him watching a show. Furthermore, due to the amount of information in a video, it is computationally unfeasible to leverage all frames of a video as context in a single forward pass. To tackle these challenges, we cast moment retrieval as a language modeling task and leverage the contextual understanding ability of generative MLLMs to interpret and comprehend the semantic and temporal action development in frames that represent a video. We first thoroughly explore the design space of timestamps in MLLMs. Our analysis resulted in our proposed recipe, *Chrono*, that can enable image-text pretrained MLLMs to interpret video frames and their respective temporal grounding in both a finetuning and even zero-shot setting. In Section 3.1, we present our proposed blueprint, *Chrono*. In Section 3.2 we discuss how our model-agnostic *Chrono* blueprint can be leveraged for adapting an MLLM using finetuning and a zero-shot setup.

3.1. Chrono blueprint

Our work investigates how to enable image-text pretrained MLLMs to comprehend video and time for temporal grounding tasks in videos given a natural language query. To do so, we cast the traditional moment retrieval task as an open-ended sequence-to-sequence problem, where we design a

novel multimodal input sequence that contains (a) the visual semantic context given the sampled frames of the video, (b) the temporal context for each event, which we model through by the temporal location of each frame (i.e., a timestamp) as well as the total video duration, and (c) the query in the form of a natural language description. The output of our model is a time interval sequence where each time interval represents a moment associated with the query and follows the formatting of a nested list of (potentially) multiple moments with a start and end time. Notably, we do not add any new special tokens and use the vocabulary native to the backbone MLLM, which allows our framework to be more general and applicable in a zero-shot setting.

To model contextual and temporal relationships between the different actions in a video and a natural language query, we cast moment retrieval as a sequence-to-sequence task and develop a novel multimodal input sequence. As illustrated in Figure 2, it consists of frames f_n , timestamps t_n ($n = 1, \dots, F$), video duration d , query q , and task prompt p stating the task at hand and, in the zero-shot setting, a format-adherence prompt, which we shown in Appendix Figure 4. Notably, there are multiple ways of representing timestamps t_n . Time can be represented in absolute or relative form, e.g., “79.9” seconds or “0.40” for a relative position (e.g. 0 being the start of the video and 1 the end); it could be a decimal number or be rounded to the nearest full integer value, e.g., “80” seconds or “40” for a relative position; the timestamps could be concatenated after the frames f_n or *interleaved* with them. As illustrated in Figure 2, we find that representing time as simple text tokens of whole seconds (integer absolute form) and interleaving them with corresponding frames yields the best performance. This finding leads to our final design for our multimodal input sequence

$$x = [f_1, r(t_1), f_2, r(t_2), \dots, f_F, r(t_F), d, q, p] \quad (1)$$

where $r(\cdot)$ represents the rounding operation. In Section 4.1, we explore the different variations of representing time and concatenation of the different sequence elements of the input.

Finally, the model is tasked to predict the sequence of potentially multiple relevant windows m , which follows the formatting of a nested list of moments with a start and end time in seconds:

$$y = [[t_{start}^1, t_{end}^1], [t_{start}^2, t_{end}^2], \dots] \quad (2)$$

Notably, this blueprint is MLLM-architecture-agnostic and can be used to adapt any image-text pretrained model through both simple finetuning and even in a zero-shot setting, which we discuss in Section 3.2.

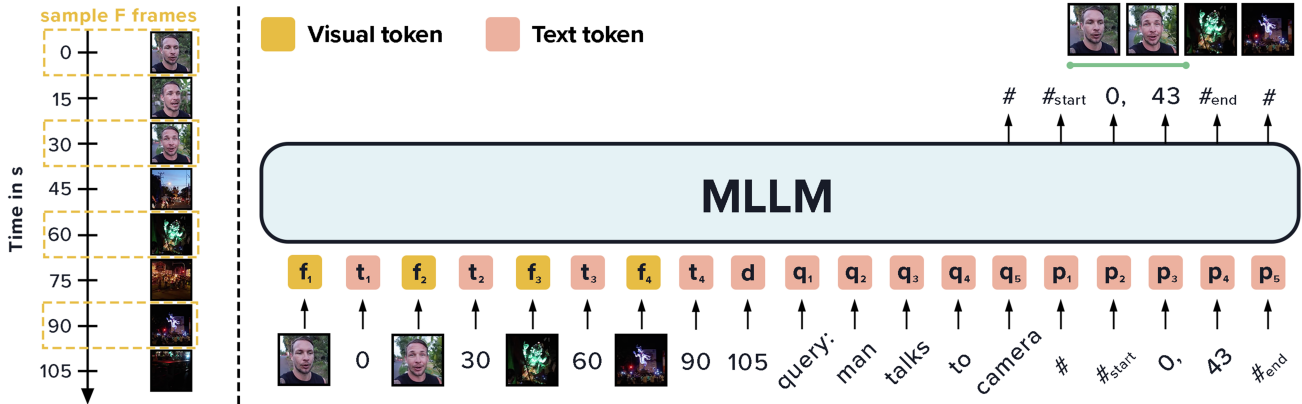


Figure 2. **Chrono** model overview. In this work, we demonstrate that our framework is model-agnostic and can adapt an image-text pretrained MLLM even in a zero-shot (no finetuning) setting. We construct the prompt for the MLLM by interleaving the frame embeddings and the timestamps of each sampled frame, followed by the video duration, the moment retrieval query, and a task prompt (the latter being not visualized.) The MLLM outputs a sequence of potentially multiple retrieved moments by predicting the global BOS and EOS tokens, denoted by #, the start of window and end of window tokens denoted as $\#_{start}$ and $\#_{end}$, and the respective start and end times for each window. In the case of finetuning a model (*Chrono-BLIP*), we freeze the MLLM and only finetune additional adapter layers leveraging parameter-efficient finetuning (Hu et al., 2022).

3.2. Training and Zero-Shot Chrono Setup

In this section, we describe two different options to apply the *Chrono* blueprint. We can either train our generative MLLM or perform zero-shot adaptation on the task of moment retrieval. We cast the traditional computer vision problem of moment retrieval as an open-ended natural language sequence-to-sequence task.

Training Setup. To train our model, we optimize for the standard maximum likelihood objective. To further optimize training and best leverage the limited video data available, we implement parameter-efficient finetuning via LoRA (Hu et al., 2022) and randomly sample video frames. This allows us to only train a fraction of the parameters of the MLLM. Additionally, by randomly sampling the frames, we optimize those weights by analyzing different frames and timestamps of the same videos each epoch. For further details, see Appendix B.2.2.

For our experiments specifically, we leverage an encoder-decoder style MLLM, BLIP-2 (Li et al., 2023). We denote BLIP-2’s frozen image encoder combined with Q-Former as our general-purpose frame encoder. The frame encoder is separately applied to each of the F sub-sampled frames, generating the frame embeddings and projecting them into the language space, yielding a shared embedding space. Prior works (Wang et al., 2024; Ren et al., 2023; Yang et al., 2023; Zhang et al., 2023b) incorporate further trainable transformer-based modules to generate temporally and contextually correlated frame- or video-level embeddings. In contrast, we solely leverage the self- and cross-attention

mechanisms of our LLM to learn the temporal and contextual relationships between frames. We coin this instantiation of the *Chrono* blueprint *Chrono-BLIP*.

Zero-Shot Setup. For zero-shot adaptation, we can apply our *Chrono* framework to an MLLM with instruction-following abilities by providing it with the video frames interleaved with their respective timestamps, the video duration, user query, and instruction prompt, just as in the training setup. The difference is that we modify the instruction prompt so that our MLLM backbone understands and solves the desired task and returns the desired format.

For our experiments, we want to demonstrate the ability of the *Chrono* blueprint on another MLLM architecture, the decoder-only architecture, and therefore select GPT-4o (OpenAI, 2024a) as our MLLM backbone of choice. We call this instantiation of our framework *Chrono-GPT* and provide the full prompt used in Appendix Figure 4.

4. Experiments

This section describes the effectiveness of our design choices and compares our method to the state-of-the-art. We validate *Chrono* on the three most widely used video moment retrieval (MR) datasets Charades-STA (Gao et al., 2017), QVHighlights (Lei et al., 2021a), and ActivityNet Captions (Krishna et al., 2017), and extend our framework to the task of grounded video questions answering on the NExT-GQA (Xiao et al., 2023) benchmark. We present and analyze the experiments in this section, with further details on our experimental setup in Appendix B.

Table 1. **Ablation studies.** We study (a) prompt components and (b) timestamp design for both our finetuned *Chrono-BLIP* and zero-shot *Chrono-GPT*. For *Chrono-BLIP*, we ablate on the Charades-STA validation set, and for *Chrono-GPT*, on the QVH validation set. D: Video Duration, T: Frame Timestamps, Rep: Representation, Rel: Relative, Abs: Absolute, Prec: Precision, Dec: Decimal, Int: Integer, Inter: Interleaved.

(a) Prompt design components						(b) Timestamp design							
		<i>Chrono-BLIP</i>		<i>Chrono-GPT</i>				<i>Chrono-BLIP</i>		<i>Chrono-GPT</i>			
D	T	R1@.5	R1@.7	R1@.5	R1@.7	Rep.	Prec.	Inter.	R1@.5	R1@.7	R1@.5	R1@.7	
						(1)	Rel	Dec	✗	62.30	37.22	48.39	26.06
✗	✗	43.84	23.95	5.74	1.94	(2)	Abs	Dec	✗	62.38	36.33	44.19	24.58
✓	✗	55.60	32.63	4.39	1.87	(3)	Rel	Int	✗	63.10	36.01	30.42	19.90
✗	✓	67.81	<u>43.33</u>	<u>60.00</u>	<u>41.68</u>	(4)	Abs	Int	✗	64.39	41.80	36.77	20.68
✓	✓	<u>67.28</u>	46.70	61.68	41.80	(5)	Rel	Int	✓	<u>65.19</u>	<u>44.94</u>	62.84	42.19
						(6)	Abs	Int	✓	67.28	46.70	<u>61.68</u>	<u>41.80</u>

4.1. Ablation Studies

By default, our *Chrono* models for Charades-STA (QVHighlights/ ActivityNet Captions) leverage 20 (60) visual frames, their associated timestamps, video duration, a query, and a task prompt. If not stated otherwise, we represent time as simple text tokens of whole seconds and interleave these with frame tokens. In the following, we ablate the impact of these design choices on the downstream moment retrieval performance by reporting results for *Chrono-BLIP* on our Charades-STA validation set and for *Chrono-GPT* on the QVHighlights validation set.

4.1.1. DESIGN OF SEQUENCE

In Table 1 (a), we analyze the effectiveness of each part of the multimodal input sequence of our MLLM by cumulatively adding each component, starting with only providing the frames. The query is always part of the sequence. For *Chrono-BLIP*, adding the video duration, in addition to the visual inputs, improves the downstream performance significantly (row 2 vs. row 1). This shows the importance of providing the model a point of reference to infer the temporal location of each frame and demonstrates the ability of the MLLM to learn this association. For *Chrono-GPT*, on the other hand, does not benefit as strongly from the additional information as our fine-tuned BLIP-2 model. Again, note that with a fixed number of uniformly sampled frames and the video duration, the model has all the information necessary to compute at which timestamp each frame was sampled. Our experiment shows that GPT-4o appears not to be able to leverage this information.

Yet, providing the specific timestamps at which each frame was sampled in an interleaved manner (as illustrated in Figure 2) improves the model performance of both our models by a significant margin (rows (3, 4) vs. rows (1,2)). This demonstrates the relevance of designing the input context to provide as much relevant information as possible while still

not relying on additional computation, such as generating and leveraging transcripts. Providing all timestamps along with the video duration yields the best performance (row 4 vs. 3) for both models.

4.1.2. DESIGN OF TIMESTAMPS

A central question for this work is how MLLMs can best represent and reason about timestamps, as they have to be interpreted in the input and predicted in the output. We compare different options for representing the timestamps and their impact on the final downstream model performance. We explore using relative positions w.r.t the video duration vs. representing each timestamp as absolute time. We compare representing these as decimal numbers (absolute “79.9” seconds, relative “0.40”) vs. integers (absolute “80” seconds, relative “40”). In these experiments, the format of the timestamps in model input and output is always consistent. In the case of relative positions, we post-process the output to yield an absolute value to compare to the ground truth for the final evaluation.

Inspecting the *Chrono-BLIP* ablations in Table 1 (b), we observe that representing the timestamps in decimal form results in lower performance for both absolute and relative form, see rows (1,2) vs. rows (3, 4). We hypothesize this is the case because of how decimal numbers are tokenized. Although using decimal timestamps allows for higher temporal resolution, we hypothesize that this lower performance can be attributed to limitations related to the tokenization of decimal numbers. Depending on the tokenizer, a decimal number such as “79.9” or “42.05” can be divided into a different number of tokens each, whereas integers (up to a certain number) are tokenized as a single token. Nevertheless, it is important to note that this behavior varies across tokenizers and can, therefore, be subject to variance. Further, we observe that absolute position in seconds yields better performance than the relative representation when using integer precision. This shows the importance of de-

signing the input and outputs with the representation of the MLLM in mind.

When analyzing the trends for *Chrono-GPT*, we find that these trends are not as evident. We observe that there are a lot of variances when evaluating *Chrono-GPT* on the downstream tasks and that it seems, when inspecting only the first four rows, that GPT-4o prefers decimal precision. We hypothesize that the GPT-4o tokenizer is more advanced and suitable for processing numbers, having a more consistent tokenization scheme. Yet, when comparing integer and decimal precision in the interleaved setting, we find that GPT-4o prefers integer precision (see Appendix Appendix C.2).

Finally, we explore the design choice of ordering frame and time tokens. In rows (1) through (4), we concatenate all frames together, followed by a concatenation of the timestamps, which are each separated by a separator token (“>”). In rows (5) and (6), we observe the benefit of *interleaving* frame tokens with time tokens when applied to both relative and absolute timestamps. For both models, *Chrono-BLIP* and *Chrono-GPT*, the most evident gain of our sequence design is that interleaving frames and timestamps significantly outperform the non-interleaved settings. Our experiments demonstrate that representing time in seconds rounded to the respective nearest integer in an interleaved sequence design yields the best performance when applied to our BLIP-2 backbone. For our *Chrono-GPT* setting, on the other hand, relative and absolute representations are on par. For the sake of simplicity and consistency in our following experimental setup, for *Chrono-GPT* we use the row 6 settings.

4.2. Comparison to the SOTA in Moment Retrieval

Next, we compare *Chrono* to the state-of-the-art (SOTA) approaches for MR following the best design choices derived from our ablations in Section 4.1. Specifically, we compare *Chrono-BLIP* to other finetuned baselines and *Chrono-GPT* to zero-shot baselines.

Firstly, in Table 2, we include a comparison to the vanilla BLIP-2 model, where we only include the frames in the context of BLIP-2 and finetune and evaluate it on each dataset, respectively. As expected, our *Chrono-BLIP* model significantly outperforms this baseline. Notably, for QVH, this improvement is less pronounced than on the other datasets because the videos in the dataset are always 150 seconds long, so the model can better learn to infer each frame’s temporal location since it is consistent. Nevertheless, it still performs far worse than our *Chrono-BLIP* model.

Compared to prior SOTA methods on QVHighlights, *Chrono-BLIP* significantly outperforms the previous SOTA InternVideo2 (Wang et al., 2024) on all metrics, which is a general video-language foundation model requiring expensive video pretraining. Our model improves the performance

by 3.35% and 4.06% for R1@0.5 and R1@0.7, respectively.

On Charades-STA, our *Chrono-BLIP* model also achieves a new state-of-the-art, improving over the previous SoTA model (Wang et al., 2024) for R1@0.7. While InternVideo2 achieves good performance by extracting intermediate features and leveraging CG-DETR (Moon et al., 2023a) as a localization head, we demonstrate strong results with a fraction of the training data, smaller model size, fewer trained parameters, and while not relying on a task-specific output head. We solely finetune on the downstream task. *Chrono-BLIP* also outperforms the previous SoTA (Yan et al., 2023) in moment retrieval on ActivityNet Captions by 5.62% and 5.35% on R1@0.5 and R1@0.7, respectively.

Our work is most comparable to SeViLa (Yu et al., 2024), which leverages the same image-text pretrained MLLM, namely BLIP-2 (Li et al., 2023), as its backbone. Our *Chrono* model achieves performance that is 20.14% and 23.29% higher than SeViLa on QVHighlights in Recall@1 at thresholds of IoU=0.5 and IoU=0.7. This demonstrates the effectiveness of our novel multimodal sequence design. Our model receives contextual and temporal information and predicts the relevant moments in consecutive autoregressive forward passes. In contrast, SeViLa classifies each frame as relevant to the query or not without any contextual and temporal information about the video.

Moreover, we also evaluate our *Chrono-GPT* model on all three MR benchmarks in a zero-shot setting. As expected, the performance achieved by *Chrono-GPT* is much lower compared to methods explicitly trained for Moment Retrieval in those same datasets. However, it performs significantly better than the baseline of only providing the frames without the *Chrono* framework, validating that our *Chrono* blueprint enables moment retrieval in a zero-shot manner. This reinforces our goal of having the simplest possible approach with competitive results, and we believe can be very useful for practitioners.

Finally, to compare to more MLLM-based MR models, we evaluate *Chrono-BLIP*’s performance on the transfer learning setting in Table 3. Prior work (Qian et al., 2024; Ren et al., 2023; Huang et al., 2024a) perform extensive video-language instruction finetuning on multiple temporal grounding datasets and evaluate the performance on the held-out Charades-STA dataset. Although the training corpus of (Qian et al., 2024) includes a subset of ActivityNet, they also evaluate on the test respective test set, whereas our transfer learning setup involves training only on QVH and then evaluating on ActivityNet Captions. For our Charades-STA evaluation, we train on ActivityNet Captions. Although these prior works train on much larger datasets and have larger model sizes, we again achieve SoTA results.

We demonstrate the surprising effectiveness of simple but

Table 2. Comparison with state-of-the-art on QVHighlights (Lei et al., 2021a), Charades-STA (Gao et al., 2017), and ActivityNet Captions (Krishna et al., 2017). † indicates QVH results are reported on the validation set.

Method	QVHighlights					Charades-STA		ActivityNet	
	R1@.5	R1@.7	mAP	mAP@.5	mAP@.75	R1@.5	R1@.7	R1@.5	R1@.7
Finetuned for Moment Retrieval									
VLG (2021)	–	–	–	–	–	–	–	46.30	29.80
SeViLa (2024)	54.50	36.50	–	–	–	–	–	–	–
CG-DETR (2023a)	65.43	48.38	42.90	64.51	42.77	58.44	36.34	–	–
UnLoc-L (2023)	–	–	–	–	–	60.80	38.40	48.30	30.20
EaTR† (2023)	61.36	45.79	41.74	61.86	41.91	68.47	44.92	–	–
InternVideo2-6B (2024)	71.42	56.45	49.24	–	–	70.03	48.95	–	–
BLIP-2 (frames only)†	69.10	46.52	37.87	60.68	38.93	43.33	32.60	25.84	9.72
<i>Chrono-BLIP</i> 🏆	74.77	60.51	51.37	68.12	53.38	69.31	49.29	53.92	35.55
Zero-Shot									
GPT-4o (frames only)†	5.49	2.17	2.81	0.76	10.56	7.02	2.12	7.20	2.80
<i>Chrono-GPT</i> 🏆 †	61.68	41.80	52.39	35.05	57.12	28.76	10.99	31.06	17.51

Table 3. Transfer Learning Results for moment retrieval across datasets. * indicates that Momentor was trained on a subset of ActivityNet Captions.

Method	Charades-STA		ActivityNet	
	R1@.5	R1@.7	R1@.5	R1@.7
Momentor* (2024)	26.60	11.60	23.00	12.40
TimeChat (2023)	32.20	13.40	–	–
VTimeLLM (2024a)	34.30	14.70	–	–
<i>Chrono-BLIP</i> 🏆	34.87	18.04	28.64	16.44

deliberate design choices for leveraging an image-text pre-trained MLLM to achieve state-of-the-art results.

4.3. Grounded Video QA on NExT-GQA

Next, we challenge *Chrono* to a new task, grounded video question answering (GQA) on the NExT-GQA (Xiao et al., 2023) benchmark, i.e., localizing a moment that is relevant to answering a question and, then even answering the question. We provide more details on the benchmark and metrics in Appendix B.

To evaluate *Chrono-BLIP* on GQA, we follow the localizer-answerer approach of SeViLa (Yu et al., 2024) using 60 frames for localizing the relevant moment, and then resampling 60 new frames out of that segment for answering the question. We apply our QVH-pretrained *Chrono-BLIP* model as the localizer and finetune a separate Flan-T5 XL LLM as our answerer. Notably, we **do not finetune** our localization model, thus applying it to a new domain, the domain of questions, where a relevant moment does not have to be explicitly described in the question to be relevant

Table 4. NExT-GQA test set. First four models are known to be explicitly finetuned on NExT-QA. See discussion in Section 4.3.

Method	mIoU	IoP@.5	A@GQA	A@QA
Finetuned on Dataset				
SeViLa (2024)	21.7	22.9	16.6	68.1
FrozenBiLM (2023)	9.6	23.7	17.5	70.8
<i>Chrono-BLIP</i> 🏆	<u>28.7</u>	<u>24.6</u>	<u>19.4</u>	<u>73.9</u>
Zero-Shot				
Uniform 60F	21.1	21.1	8.7	7.1
LLoVi (2023a)	21.5	38.0	26.8	-
DeVi (2024)	20.7	33.8	26.9	70.9
<i>Chrono-GPT</i> 🏆	36.5	50.8	42.1	79.3

to answering it. We also compare to uniformly sampling 60 frames. Table 4 demonstrates the performance of *Chrono-BLIP* on the NExT-GQA (Xiao et al., 2023) benchmark and compares it to prior state-of-the-art models, SeViLa and FrozenBiLM (NG+) (Xiao et al., 2023).

Inspecting the mIoU scores, we can see that we outperform the FrozenBiLM model by 19.13%. In fact, on the mIoU, FrozenBiLM and SeViLa are performing worse or on par with the uniform baseline, respectively. Both *Chrono-BLIP* (localizer) and SeViLa’s localizer were pretrained solely on QVH. Yet, *Chrono-BLIP* adapts much better to the new question-based setting by achieving a 7.03% higher mIoU than SeViLa. Finally, *Chrono-BLIP* outperforms the prior SOTA by 1.90% on the A@GQA metric.

Following the same protocol, we evaluate our *Chrono-GPT* model in a zero-shot setting. As ablated, our timestamp design enables strong zero-shot moment retrieval for *Chrono-*

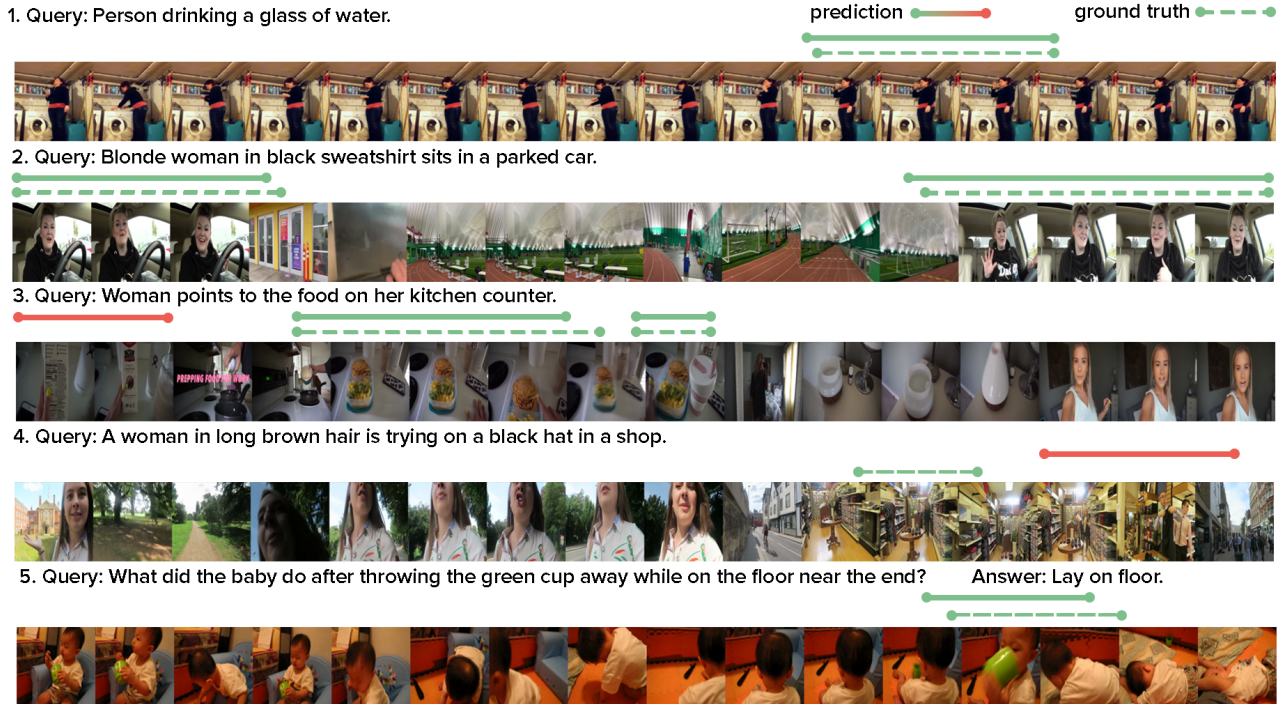


Figure 3. (1,2) correct multi-window moment retrieval. (3) *Chrono-BLIP* predicts two correct moments alongside one that is false. (4) *Chrono-BLIP* predicts a moment that only partly matches the query. (5) *Chrono-BLIP* successfully predicts an out-of-distribution example on NExT-GQA while being trained on QVH. (1) is from Charades-STA, (2) to (4) are from QVHighlights, and (5) is from NExT-GQA.

GPT. Paired with the strong QA abilities of a foundational model, we achieve a new state-of-the-art result on NExT-GQA over prior work (Zhang et al., 2023a; Qin et al., 2024), which also leverages GPT-4 and GPT-4o, respectively.

We detail our setup for NExT-GQA with *Chrono-GPT*, alongside ablations for various design decisions, in Appendix Appendix C.3.

4.4. Qualitative Results

Figure 3 shows qualitative results that demonstrate *Chrono-BLIP*’s ability to predict multiple windows (2 and 3), generalize to unseen data distributions (5), as well as some failure modes like predicting wrong segments (3) and only partially adhering to the prompt due to low image resolution (4). In (4), the query is ”A woman in long brown hair is trying on a black hat in a shop”. *Chrono-BLIP* predicts a moment where the woman is clearly visible in a shop but not trying on a hat. In the ground truth segment, the woman is trying on a hat but is not clearly visible since she is far away. We provide more videos with localizations in Appendix D.

5. Conclusion

We introduce *Chrono*, a simple model-agnostic blueprint for providing temporal information to video-language MLLMs, thus enabling them to perform tasks such as mo-

ment retrieval and grounded video question answering. We show that originally image-text pretrained *Chrono* models can easily adapt to the video-language modality and greatly benefit from an input design that incorporates visual and temporal information as a simple interleaved token sequence of visual and text tokens. Specifically, finetuned *Chrono-BLIP* achieves state-of-the-art results on the popular moment retrieval benchmarks, whereas zero-shot *Chrono-GPT* achieves a new SoTA in grounded video question answering. Through our extensive ablations, we surprisingly find that our simple model-agnostic design outperforms all prior SOTA methods, which rely on aspects like task-specific model architectures, extensive video pretraining, further input signal, such as video transcripts or novel time embedding modules. We hope this versatile sequence-to-sequence design of *Chrono* serves as a fundamental baseline or potential best practice for encoding time in video-language models and sparks further research in leveraging image-text pretrained MLLMs for video understanding tasks.

6. Limitations and Impact

Since we leverage large-scale pretrained MLLMs, BLIP-2 (Li et al., 2023) and GPT-4o (OpenAI, 2024a), we can not rule out the presence of biases or harmful stereotypes (e.g., gender or racial biases) that these models have learned. It is conceivable that our model will detect moments that fall

into the category of harmful stereotypes. We recommend applying our model with caution when adopting it in practice. Moreover, our model could be subject to misuse w.r.t some forms of surveillance.

7. Acknowledgements

The research was partially funded by a LOEWE-Start-Professur (LOEWE/4b//519/05.01.002-(0006)/94), LOEWE-Spitzen-Professur (LOEWE/ 4a//519/05.00.002-(0010)/93) and an Alexander von Humboldt Professorship in Multimodal Reliable AI, sponsored by Germany’s Federal Ministry for Education and Research.

References

- Alayrac, J.-B., Donahue, J., Luc, P., Miech, A., Barr, I., Hasson, Y., Lenc, K., Mensch, A., Millican, K., Reynolds, M., et al. Flamingo: a visual language model for few-shot learning. In *Advances in Neural Information Processing Systems*, volume 35, pp. 23716–23736, 2022.
- Anne Hendricks, L., Wang, O., Shechtman, E., Sivic, J., Darrell, T., and Russell, B. Localizing moments in video with natural language. In *Proceedings of the IEEE international conference on computer vision*, pp. 5803–5812, 2017.
- Brown, T., Mann, B., Ryder, N., Subbiah, M., Kaplan, J. D., Dhariwal, P., Neelakantan, A., Shyam, P., Sastry, G., Askell, A., et al. Language models are few-shot learners. In *Advances in neural information processing systems*, volume 33, pp. 1877–1901, 2020.
- Cao, M., Yang, T., Weng, J., Zhang, C., Wang, J., and Zou, Y. Locvtp: Video-text pre-training for temporal localization. In *European Conference on Computer Vision*, pp. 38–56. Springer, 2022.
- Chen, J., Chen, X., Ma, L., Jie, Z., and Chua, T.-S. Temporally grounding natural sentence in video. In *Proceedings of the 2018 conference on empirical methods in natural language processing*, pp. 162–171, 2018.
- Chung, H. W., Hou, L., Longpre, S., Zoph, B., Tay, Y., Fedus, W., Li, Y., Wang, X., Dehghani, M., Brahma, S., et al. Scaling instruction-finetuned language models. *arXiv preprint arXiv:2210.11416*, 2022.
- Fang, H., Xiong, P., Xu, L., and Chen, Y. Clip2video: Mastering video-text retrieval via image clip. *arXiv preprint arXiv:2106.11097*, 2021.
- Fang, H., Xiong, P., Xu, L., and Luo, W. Transferring image-clip to video-text retrieval via temporal relations. *IEEE Transactions on Multimedia*, 2022.
- Feichtenhofer, C., Fan, H., Malik, J., and He, K. Slowfast networks for video recognition. In *Proceedings of the IEEE/CVF international conference on computer vision*, pp. 6202–6211, 2019.
- Gao, J., Sun, C., Yang, Z., and Nevatia, R. Tall: Temporal activity localization via language query. In *Proceedings of the IEEE international conference on computer vision*, pp. 5267–5275, 2017.
- Hu, E. J., Shen, Y., Wallis, P., Allen-Zhu, Z., Li, Y., Wang, S., Wang, L., and Chen, W. Lora: Low-rank adaptation of large language models. In *International Conference on Learning Representations*, 2022.
- Huang, B., Wang, X., Chen, H., Song, Z., and Zhu, W. Vtimellm: Empower llm to grasp video moments. In *Proceedings of the IEEE/CVF Conference on Computer Vision and Pattern Recognition (CVPR)*, pp. 14271–14280, June 2024a.
- Huang, D.-A., Liao, S., Radhakrishnan, S., Yin, H., Molchanov, P., Yu, Z., and Kautz, J. Lita: Language instructed temporal-localization assistant. In *European Conference on Computer Vision*, pp. 202–218. Springer, 2025.
- Huang, S., Dong, L., Wang, W., Hao, Y., Singhal, S., Ma, S., Lv, T., Cui, L., Mohammed, O. K., Patra, B., et al. Language is not all you need: Aligning perception with language models. In *Advances in Neural Information Processing Systems*, volume 36, 2024b.
- Jang, J., Park, J., Kim, J., Kwon, H., and Sohn, K. Knowing where to focus: Event-aware transformer for video grounding. In *Proceedings of the IEEE/CVF International Conference on Computer Vision*, pp. 13846–13856, 2023.
- Ju, C., Han, T., Zheng, K., Zhang, Y., and Xie, W. Prompting visual-language models for efficient video understanding. In *European Conference on Computer Vision*, pp. 105–124. Springer, 2022.
- Krishna, R., Hata, K., Ren, F., Fei-Fei, L., and Carlos Niebles, J. Dense-captioning events in videos. In *Proceedings of the IEEE international conference on computer vision*, pp. 706–715, 2017.
- Lee, P. and Byun, H. Bam-detr: Boundary-aligned moment detection transformer for temporal sentence grounding in videos. *arXiv preprint arXiv:2312.00083*, 2023.
- Lei, J., Berg, T. L., and Bansal, M. Detecting moments and highlights in videos via natural language queries. In *Advances in Neural Information Processing Systems*, volume 34, pp. 11846–11858, 2021a.

- Lei, J., Li, L., Zhou, L., Gan, Z., Berg, T. L., Bansal, M., and Liu, J. Less is more: Clipbert for video-and-language learning via sparse sampling. In *Proceedings of the IEEE/CVF conference on computer vision and pattern recognition*, pp. 7331–7341, 2021b.
- Lei, J., Berg, T. L., and Bansal, M. Revealing single frame bias for video-and-language learning. In *Annual Meeting of the Association for Computational Linguistics*, 2022.
- Li, J., Li, D., Savarese, S., and Hoi, S. Blip-2: bootstrapping language-image pre-training with frozen image encoders and large language models. In *Proceedings of the 40th International Conference on Machine Learning, ICML'23*. JMLR.org, 2023.
- Liu, Y., Li, S., Wu, Y., Chen, C.-W., Shan, Y., and Qie, X. Umt: Unified multi-modal transformers for joint video moment retrieval and highlight detection. In *Proceedings of the IEEE/CVF Conference on Computer Vision and Pattern Recognition*, pp. 3042–3051, 2022.
- Loshchilov, I. and Hutter, F. Decoupled weight decay regularization. *arXiv preprint arXiv:1711.05101*, 2017.
- Luo, H., Ji, L., Zhong, M., Chen, Y., Lei, W., Duan, N., and Li, T. Clip4clip: An empirical study of clip for end to end video clip retrieval and captioning. *Neurocomputing*, 508:293–304, 2022.
- Ma, Y., Xu, G., Sun, X., Yan, M., Zhang, J., and Ji, R. X-clip: End-to-end multi-grained contrastive learning for video-text retrieval. In *Proceedings of the 30th ACM International Conference on Multimedia*, pp. 638–647, 2022.
- Moon, W., Hyun, S., Lee, S., and Heo, J.-P. Correlation-guided query-dependency calibration in video representation learning for temporal grounding. *arXiv preprint arXiv:2311.08835*, 2023a.
- Moon, W., Hyun, S., Park, S., Park, D., and Heo, J.-P. Query-dependent video representation for moment retrieval and highlight detection. In *Proceedings of the IEEE/CVF Conference on Computer Vision and Pattern Recognition*, pp. 23023–23033, 2023b.
- Mun, J., Cho, M., and Han, B. Local-global video-text interactions for temporal grounding. In *Proceedings of the IEEE/CVF Conference on Computer Vision and Pattern Recognition*, pp. 10810–10819, 2020.
- OpenAI. Gpt-4o system card. Technical report, OpenAI, 2024a. URL <https://cdn.openai.com/gpt-4o-system-card.pdf>.
- OpenAI. Gpt-4 technical report, 2024b. URL <https://arxiv.org/abs/2303.08774>.
- Qian, L., Li, J., Wu, Y., Ye, Y., Fei, H., Chua, T., Zhuang, Y., and Tang, S. Momentor: Advancing video large language model with fine-grained temporal reasoning. In *Forty-first International Conference on Machine Learning, ICML 2024, Vienna, Austria, July 21-27, 2024*. OpenReview.net, 2024. URL <https://openreview.net/forum?id=e3geukCBw6>.
- Qin, H., Xiao, J., and Yao, A. Question-answering dense video events. *ArXiv*, abs/2409.04388, 2024. URL <https://api.semanticscholar.org/CorpusID:272463859>.
- Radford, A., Kim, J. W., Hallacy, C., Ramesh, A., Goh, G., Agarwal, S., Sastry, G., Askell, A., Mishkin, P., Clark, J., et al. Learning transferable visual models from natural language supervision. In *International conference on machine learning*, pp. 8748–8763. PMLR, 2021.
- Ren, S., Yao, L., Li, S., Sun, X., and Hou, L. Timechat: A time-sensitive multimodal large language model for long video understanding. *2024 IEEE/CVF Conference on Computer Vision and Pattern Recognition (CVPR)*, pp. 14313–14323, 2023. URL <https://api.semanticscholar.org/CorpusID:265608767>.
- Soldan, M., Xu, M., Qu, S., Tegner, J., and Ghanem, B. Vlg-net: Video-language graph matching network for video grounding. In *Proceedings of the IEEE/CVF International Conference on Computer Vision*, pp. 3224–3234, 2021.
- Wang, J., Ma, L., and Jiang, W. Temporally grounding language queries in videos by contextual boundary-aware prediction. In *Proceedings of the AAAI Conference on Artificial Intelligence*, volume 34, pp. 12168–12175, 2020.
- Wang, J., Ge, Y., Cai, G., Yan, R., Lin, X., Shan, Y., Qie, X., and Shou, M. Z. Object-aware video-language pre-training for retrieval. In *Proceedings of the IEEE/CVF conference on computer vision and pattern recognition*, pp. 3313–3322, 2022.
- Wang, Y., Li, K., Li, X., Yu, J., He, Y., Chen, G., Pei, B., Zheng, R., Wang, Z., Shi, Y., Jiang, T., Li, S., Xu, J., Zhang, H., Huang, Y., Qiao, Y., Wang, Y., and Wang, L. Internvideo2: Scaling foundation models for multimodal video understanding. In *European Conference on Computer Vision*, 2024. URL <https://api.semanticscholar.org/CorpusID:271432386>.
- Xiao, J., Shang, X., Yao, A., and seng Chua, T. Next-qa: Next phase of question-answering to explaining temporal actions. *2021 IEEE/CVF Conference on Computer Vision and Pattern Recognition (CVPR)*, pp. 9772–9781,

2021. URL <https://api.semanticscholar.org/CorpusID:234763093>.
- Xiao, J., Yao, A., Li, Y., and Chua, T.-S. Can i trust your answer? visually grounded video question answering. *2024 IEEE/CVF Conference on Computer Vision and Pattern Recognition (CVPR)*, pp. 13204–13214, 2023. URL <https://api.semanticscholar.org/CorpusID:261531601>.
- Xu, H., Ye, Q., Yan, M., Shi, Y., Ye, J., Xu, Y., Li, C., Bi, B., Qian, Q., Wang, W., et al. mplug-2: A modularized multi-modal foundation model across text, image and video. In *International Conference on Machine Learning*, pp. 38728–38748. PMLR, 2023.
- Xue, H., Sun, Y., Liu, B., Fu, J., Song, R., Li, H., and Luo, J. Clip-vip: Adapting pre-trained image-text model to video-language representation alignment. In *International Conference on Learning Representations*, 2023.
- Yan, S., Xiong, X., Nagrani, A., Arnab, A., Wang, Z., Ge, W., Ross, D., and Schmid, C. Unloc: A unified framework for video localization tasks. In *Proceedings of the IEEE/CVF International Conference on Computer Vision*, pp. 13623–13633, 2023.
- Yang, A., Nagrani, A., Seo, P. H., Miech, A., Pont-Tuset, J., Laptev, I., Sivic, J., and Schmid, C. Vid2seq: Large-scale pretraining of a visual language model for dense video captioning. In *Proceedings of the IEEE/CVF Conference on Computer Vision and Pattern Recognition*, pp. 10714–10726, 2023.
- Yu, K. P., Zhang, Z., Hu, F., and Chai, J. Efficient in-context learning in vision-language models for egocentric videos. *arXiv preprint arXiv:2311.17041*, 2023.
- Yu, S., Cho, J., Yadav, P., and Bansal, M. Self-chained image-language model for video localization and question answering. In *Advances in Neural Information Processing Systems*, volume 36, 2024.
- Zeng, R., Xu, H., Huang, W., Chen, P., Tan, M., and Gan, C. Dense regression network for video grounding. In *Proceedings of the IEEE/CVF Conference on Computer Vision and Pattern Recognition*, pp. 10287–10296, 2020.
- Zhang, C., Lu, T., Islam, M. M., Wang, Z., Yu, S., Bansal, M., and Bertasius, G. A simple llm framework for long-range video question-answering. In *Findings of the Association for Computational Linguistics: EMNLP 2024*, volume abs/2312.17235, 2023a. URL <https://api.semanticscholar.org/CorpusID:266573523>.
- Zhang, H., Li, X., and Bing, L. Video-LLaMA: An instruction-tuned audio-visual language model for video understanding. In Feng, Y. and Lefever, E. (eds.), *Proceedings of the 2023 Conference on Empirical Methods in Natural Language Processing: System Demonstrations*, pp. 543–553, Singapore, December 2023b. Association for Computational Linguistics.
- Zhang, S., Roller, S., Goyal, N., Artetxe, M., Chen, M., Chen, S., Dewan, C., Diab, M., Li, X., Lin, X. V., et al. Opt: Open pre-trained transformer language models. *arXiv preprint arXiv:2205.01068*, 2022.

A. Appendix Overview

In the Appendix, we elaborate on further details of our work and present additional experiments. Specifically, we discuss the following:

- Our experimental setup, detailing the benchmarks we used and our training and zero-shot setup details for reproducibility in Appendix B.
- Ablations on the effect of the number of trainable parameters in Appendix C.1.
- In Appendix C.2, further detailed ablations on the timestamp design for zero-shot GPT-4o on Charades-STA (Table 7) and QVHighlights (Table 8). We find that for longer videos, the effect of interleaving the timestamps greatly improves the moment localization performance, supporting our findings in the main paper.
- The exact prompt used for querying GPT-4o (Figure 4).
- Additional qualitative examples (Appendix D).
- Finally, we provide a separate video montage showcasing example videos from the benchmarks and *Chrono-BLIP*'s predicted moment localizations and the code, respectively.

B. Experimental Setup

B.1. Benchmarks

Charades-STA (Gao et al., 2017) includes 9,848 videos with an average duration of 30.6 seconds. The dataset contains 16,128 annotations with an average moment length of 8.1 seconds and an average query length of 7.22 words. The dataset is originally divided into two splits: training (12,408) and test (3,720). To avoid overfitting on the test set during training, we designate a part of the training set as a new validation set. The videos used in the validation set are not contained in the training set. Our new dataset split consists of a split for training, validation, and testing, with 11,166, 1,242, and 3,720 annotations, respectively. For a fair comparison, after completing our ablations, we train our final model on the original training set and report numbers on the test set. We will share our split for reproducibility.

QVHighlights (Lei et al., 2021a) is one of the most recent benchmarks and contains 10,148 videos with a duration of 150 seconds. The videos were cropped out of YouTube videos, and each video is annotated with at least one query with an average length of 11.3 words describing the relevant moment. The target windows have an average length of 24.6 seconds. The dataset is split into training, validation, and test sets with 7,218, 1,150, and 1,542 queries, respectively. This benchmark is challenging because one query can be associated with multiple moments in a video. The test set targets are withheld and thus guarantee a fair benchmark. The evaluation for the test split can only be measured through submitting the prediction to the evaluation server⁵.

ActivityNet Captions (Krishna et al., 2017) contains 20,000 videos with an average duration of 2 minutes. The dataset contains 72,000 segments, each human-annotated with a caption that includes, on average, 13.5 words. The dataset is divided into three splits, train (37,421), val_1 (17,505), and val_2 (17,031). Following (Yan et al., 2023), we use the train split for training, val_1 for validation, and val_2 for testing.

NExT-GQA (Xiao et al., 2023) extends the NExT-QA (Xiao et al., 2021) benchmark by providing temporal grounding for the moments in the video, that are relevant for answering the question for the validation and test sets, making this a weakly-supervised dataset. The dataset contains the original training split of NExT-QA, which includes 34,132 samples. The validation set contains 3,358 questions with 3,931, meaning a sample can potentially have multiple relevant moments, but where predicting any single one of those moments is a correct prediction, i.e., one does not have to predict all relevant moments. The test set has 5,553 questions with 6,600 segments. The segments have an average duration of 7.3 and 6.7 seconds for the validation and test set, respectively.

⁵Eval server: <https://codalab.lisn.upsaclay.fr/competitions/6937>

B.1.1. METRICS

The most commonly used metrics for MR are Recall@K and mean average precision (mAP) computed under different Intersection over Union (IoU) thresholds. The Recall@K metric is defined as the percentage of the top-K predicted segments having a larger temporal IoU than the threshold with a ground truth segment. Following the recent development (Lee & Byun, 2023; Lei et al., 2021a; Moon et al., 2023a;b), we report the more challenging $R1@0.5$ and $R1@0.7$ scores, which correspond to the $Recall@1$ scores at IoU thresholds of 0.5 and 0.7, respectively, and the mean IoU (mIoU) score. Following these prior works, for MR on QVHighlights, we report the mAP score at IoU thresholds of 0.5 and 0.75 and the average mAP, respectively.

NExT-GQA (Xiao et al., 2023) introduces the metrics (i) *Intersection over Prediction (IoP)*, which is defined as the ratio between the length of the temporal intersection between the predicted relevant moment and ground truth and the length of the predicted moment itself, and (ii) *Accuracy@GQA (A@GQA)* which is the accuracy of correctly answered questions that have a grounding score of $IoP > 0.5$. The IoP loosens the common IoU metric by only considering the intersection over the length of the prediction instead of over the union. This metric encourages very short-moment predictions and is not concerned with a precise coverage of the entire relevant moment.

B.2. Implementation Details

In this section, we present the specific finetuning and evaluation details for *Chrono-BLIP*, as well as further specific zero-shot evaluation elements for *Chrono-GPT*

B.2.1. TRAINING DETAILS FOR BLIP2

Considering the relatively small scale of the datasets, we choose not to finetune the entire 3 billion parameter-LLM backbone of our model but rather leverage parameter-efficient finetuning (Hu et al., 2022) to train only 19 million parameters, as described in Section 3.2.

Since our objective is a generative language modeling task, our model can output minor formatting inconsistencies that would invalidate the prediction if not treated otherwise. Similar to (Yang et al., 2023), we post-process the model’s outputs by applying heuristics to clean up minor flaws in the prediction.

For Charades-STA, we extract 20 video frames for each video, which is significantly less than prior work (Yan et al., 2023), which requires 128 frames. We train for up to 20 epochs with a batch size of 32 samples split across 4 A100-80GB GPUs for about 20 GPU hours. For QVHighlights and ActivityNet Captions, we extract 60 video frames for each video, which is less than required by prior work (Moon et al., 2023a;b). We train for up to 50 epochs with an effective batch size of 32 samples by splitting them across 8 A100-80-GB GPUs and leveraging accumulated gradients set to 4 (i.e., we have one sample per GPU) and train for about 170 GPU hours.

We start with a learning rate (lr) of $1e-8$, perform linear lr warmup to $3e-4$ for 10% of the total number of iterations, and then apply a cosine lr decay. We utilize the AdamW (Loshchilov & Hutter, 2017) optimizer and sample the frames randomly during training.

B.2.2. VIDEO PROCESSING

We build on top of the Salesforce *lavis* repository and leverage their implementation of randomly and uniformly extracting frames from a video. During training, we randomly sample frames as a means of data augmentation to alter the frames seen by the model in each batch. At inference, we sample uniformly to provide an equal coverage of the entire video. For random sampling, we start by uniformly extracting $n+1$ timestamps, where the first and last timestamps are at $t = 0$ and $t = video_length$, respectively. Afterward, we randomly sample one frame between each pair of adjacent timestamps, yielding the final n randomly sampled frames. This process of random sampling can be considered adding noise to a uniform sampling process.

During training, we randomly crop and resize each frame to 224x224 pixels. We then normalize each frame by subtracting by a fixed mean and dividing by a specified standard deviation. At inference, we don’t apply random cropping and resizing. We only apply the normalization.

Table 5. Hyperparameters for our base models for Charades-STA (Gao et al., 2017), QVHighlights (QVH) (Lei et al., 2021a), and ActivityNet (ANet) (Krishna et al., 2017) and for training of the answerer for NeXT-GQA (Xiao et al., 2023). LR: Learning rate.

Hyperparameter	Charades-STA	QVH/ ANet/ NeXT-GQA
Batch size	32	32
Epochs	20	50
LR	3e-4	3e-4
LR warmup	Linear	Linear
LR warmup steps	10%	10%
LR decay	Cosine	Cosine
Optimizer	AdamW	AdamW
Weight decay	0.05	0.05
# input frames	20	60
# beams	5	5

Table 6. Ablation on the LoRA Rank and number of trainable parameters.

Rank (# train. params)	R1@0.5	R1@0.7	mIoU
2 (6M)	66.03	43.03	56.59
4 (10M)	65.71	43.59	56.78
8 (19M)	67.28	46.70	57.46
16 (37M)	67.72	45.38	57.35

B.2.3. FINETUNING HYPERPARAMETERS

Table 5 shows a detailed list of hyperparameters. To ensure a fair comparison for all our models and ablations, we stick to hyperparameters presented in the table, except for the cases where we ablate certain parameters (Table 1). The only hyperparameters that change across benchmarks are the number of steps for the learning rate warmup and the number of input frames. The number of warmup steps depends on the dataset size and corresponds to 10% of the total number of steps, i.e.

$$\#steps_{warmup} = 0.1 * \#steps/epoch * \#epochs \quad (3)$$

B.2.4. ZERO-SHOT GPT-4O EXPERIMENT DETAILS

We query *gpt-4o-2024-08-06* through the API. We use *low* image details for all queries. It is likely that with *high* image details, the results would be better, as more tokens are devoted per image, but we didn’t explore it in detail. We use temperature zero and maximum generation length for all the queries and use other API parameters as default. We observe some non-determinism even when using temperature 0, but all the results are statistically significant and, when possible, are averaged over at least two runs.

C. Additional Ablations

C.1. Effect of number of trainable parameters

In the main paper, we state the use of parameter-efficient finetuning techniques and thus training only a small number of parameters. In practice, we leverage LoRA (Hu et al., 2022) with a rank set to 8 and apply it to all linear layers in the large language model, yielding about 19 million trainable parameters.

In Table 6, we show the effect of different LoRA ranks and their resulting number of trainable parameters. We observe that setting the rank to 16, i.e. training double the number of parameters does not yield any significant improvement (row 4). Moreover, training fewer parameters, i.e. 10 or 6 million, by setting the rank to 4 or 2, respectively, does degrade the performance of *Chrono* (rows 1 and 2).

Table 7. Ablation studies on Charades-STA Validation set. Effect of timestamp design on zero-shot evaluation using GPT-4o.

#	Rep.	Prec.	Inter.	R1@0.5	R1@0.7	mIoU
(1)	Rel	Dec	✗	32.85	11.38	37.78
(2)	Abs	Dec	✗	32.38	13.30	36.99
(3)	Rel	Int	✗	34.68	15.46	38.04
(4)	Abs	Int	✗	29.91	11.28	33.43
(5)	Rel	Int	✓	34.86	11.20	38.44
(6)	Abs	Int	✓	28.35	11.29	35.43
(7)	Abs	Dec	✓	28.72	10.74	34.78

Table 8. Ablation studies on QVHighlights Validation set. Effect of timestamp design on zero-shot evaluation using GPT-4o.

#	Rep.	Prec.	Inter.	R1@0.5	R1@0.7	mIoU
(1)	Rel	Dec	✗	48.39	26.06	46.45
(2)	Abs	Dec	✗	44.19	24.58	43.82
(3)	Rel	Int	✗	30.42	14.90	33.91
(4)	Abs	Int	✗	36.77	20.68	37.41
(5)	Rel	Int	✓	62.84	42.19	57.91
(6)	Abs	Int	✓	61.68	41.80	57.12
(7)	Abs	Dec	✓	58.77	40.16	55.83

C.2. Timestamp design for GPT-4o

Tables 7 and 8 show our ablations on zero-shot prompting GPT-4o (using the prompt shown in Figure 4) with different timestamp representations, precision, and whether we interleave them with the frames or not. Table 8 supports our main hypothesis, that interleaving timestamps between frames leads to better localisation, also in the zero-shot case.

The effect of interleaving is less clear with Charades-STA, as shown in Table 7. We hypothesize that this difference is caused by the fact that we use only 20 frames (out of shorter videos) for Charades-STA, whereas in the QVHighlights, GPT-4o observes 60 frames (of videos up to several minutes long). This means appended timestamps are further away from the frame that they refer to, making the gap larger to interleaving frame timestamps in Table 8. However, in Charades-STA, the shorter distance between token frames and appended timestamps seemingly has a smaller effect. Additionally, we could hypothesize that successive frames are more in distribution for GPT-4o than a series of frames with interleaved timestamps, therefore offering some benefit to simply appending the timestamps in very short frame sequences. This illustrates how some timestamp decisions that are easier to learn and used if finetuned on, as shown for *Chrono*, might be more out-of-distribution and hence less performant when used with models zero-shot. To a smaller degree, we can also observe a similar trend regarding relative versus absolute timestamps. The preference for the former is higher in shorter videos but still maintains for longer ones. We hypothesize that this better performance of relative timestamps in Charades-STA might be caused by relative timestamps offering higher temporal resolution in shorter videos. Ultimately, although absolute timestamps might be better when finetuned, as we showed for *Chrono*, we find that relative timestamps are comparable or better when using GPT-4o zero-shot. Lastly, the best configurations for both datasets use integer precision rather than decimal, even if the latter offers a higher temporal resolution, which is in agreement with the results when finetuning, as shown in Table 1.

These findings demonstrate the relevance of deliberate sequence design for different MLLMs in zero-shot and finetuned settings and its effect on enabling MLLMs for temporal localization in videos.

C.3. Chrono design for NExT-GQA

The best *Chrono-GPT* setup for NExT-GQA uses a single stage, i.e., asks for grounding and question answering in the same model response. We find that this performs better than 2 stages, where the model first performs moment retrieval, and then the model is asked to answer the question. This is the case even when the second stage is able to zoom in on the window, use more frames overall, and keep the first stage in context. We choose to use 1.4FPS for the final results. This uses an equivalent number of frames across the entire dataset (with an average length of around 40 seconds) compared to using 60

Table 9. Does moment retrieval help Video QA? We randomly choose 1000 samples from NExT-GQA validation split. We test whether asking the model to perform moment retrieval simultaneously to answering the question improves accuracy. We test whether timestamping the frames has an effect on this. *Chrono-GPT* uses interleaved timestamps with absolute time. All models use a single stage with 1.4FPS.

MR	Time	mIoU	mIoP	IoP@.5	A@GQA	A@QA
✗	✗	-	-	-	-	79.80
✓	✗	22.47	29.85	27.13	22.03	80.07
✓	✓	37.02	51.62	52.45	43.35	80.15

frames for every video. Using absolute interleaved timestamps significantly improves temporal grounding and, therefore, grounded accuracy. It modestly helps overall accuracy, i.e., not thresholded by grounding, as can be seen also in Table 9. This could indicate that including temporal grounding capabilities into models that process video cannot only offer greater interpretability but also improve their overall performance at other tasks like video QA.

User

[Frame at t_1 seconds: f_1] [Frame at t_2 seconds: f_2] [...] [Frame at F seconds: f_F]

The video lasts `duration` seconds.

Query: `query`.

Given the video and the query, find the relevant windows. Think step by step. Reason about the events in the video and how they relate to the query. After your reasoning, output ‘ANSWER: <your answer>’ in the format specified in the task prompt. Always provide a non-empty answer after your thoughts. If you think the event does not take place in the video, give your best guess, as otherwise the evaluation will be marked as incorrect. Never provide an empty list for <your answer>. The descriptions of moments are sometimes imprecise, so retrieve the closest moment. If you don’t see an event remotely similar to the description, guess what is the most likely moment given the context. For instance, for cutting onion this could be between the time we see that the scene takes place in the kitchen and the time we see the onions being boiled in the pan. The answer should be in the format of a list indicating the start and end of a window of moment, [start_window, end_window], for instance [0, 1]. If you detect multiple windows for the same moment, choose the most relevant one. It’s important your final answer only contains one window. It is very important that the answer is in this format, otherwise the evaluation will fail.

Assistant

`Answer`

Figure 4. Prompt used for GPT-4o for single-window moment localization. Blue text represents variables.

D. Additional Qualitative Results

In this section, we provide further qualitative results and discuss shortcomings of our model that can be addressed in future research. For each example, we provide the discussion in the respective caption for the convenience of the reader. Examples 1 through 6 are from QVHighlights (Lei et al., 2021a) and examples 6 through 10 are from Charades-STA (Gao et al., 2017).

As in the main paper, we illustrate the ground truth targets as dashed lines and the predicted windows as solid lines.

A girl is excited about showing her bed with a big red heart in it.



Figure 5. We observe the capability of our model to recognize and differentiate 3 separate moments that repeatedly occur with intermittent interruptions. Each predicted moment depicts the respective natural language query.

Donald Trump speaks in large circular table.



Figure 6. Chrono-BLIP can recognize a distinct public figure, Donald Trump, although the training set includes only 6 queries containing Donald Trump.

Man and woman sit on opposite sides of circle desk.



Figure 7. Our model predicts a third window, that does not align with a ground truth moment, which, in fact, is accurate and depicts the query.

Soldiers escort people through the wilderness.



Figure 8. The video contains two groups of relevant moments which contain a short sub-2-second cut that does not depict the query. With a resolution of 60 frames for a 150-second long video, corresponding to a frame being seen every 2.5 seconds, Chrono-BLIP can not detect the cut and predicts two long moments that encompass the two short ones. Moreover, our model predicts a third window (red) that does not match a ground truth label. The predicted moment does in actuality depict soldiers, but those are not escorting other people.

A herd of bison is shown crossing the road.



Figure 9. Our model has trouble predicting very short moments in long videos and high-frequency jump cuts given the resolution of the frame sampling.

a person awakens in a bedroom.

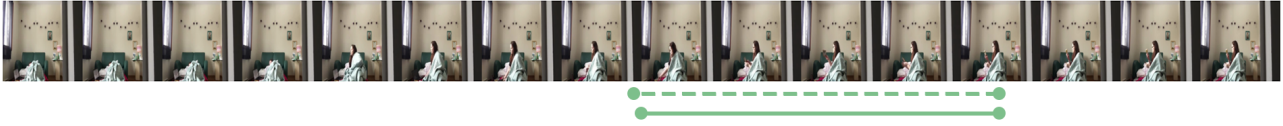


Figure 10. Given a very ambiguous query, our model's prediction aligns with the ground truth.

a person closes a front door.



Figure 11. Our model fails to recognize the action of the man closing the front door. We hypothesize this is because the door is very dark and poorly visible. Our model predicts the moment when the door is clearly visible and closed.

the person puts the broom down.



Figure 12. Our model fails to recognize the action of putting down the broom at the beginning of the video and predicts the moment when the man picks the broom back up and then holds it.

the person begins sneezing.



Figure 13. Chrono-BLIP recognizes the moment when the person is sneezing. The ground truth is false.